

## Anomalous softening of order parameter fluctuations at the smectic-A to -C\* transition in a siloxane-substituted chiral liquid crystal

A. Tang,<sup>1</sup> D. Konovalov,<sup>1</sup> J. Naciri,<sup>2</sup> B. R. Ratna,<sup>2</sup> and S. Sprunt<sup>1</sup>

<sup>1</sup>Department of Physics, Kent State University, Kent, Ohio 44242

<sup>2</sup>Center for Biomolecular Science and Engineering, Code 6900, Naval Research Laboratory, Washington, DC 20375-5348

(Received 9 April 2001; published 17 December 2001)

Unconventional softening of order-parameter fluctuations is observed at the smectic-A to smectic-C\* phase transition in a chiral liquid crystal possessing multiple siloxane substituents on its hydrocarbon chains. Together with an optical “stripe” texture detected above the transition, the atypical dynamics can be explained by the pretransitional development within the smectic layers of a modulated state of the order parameter. Conventional soft-mode behavior is restored when the degree of chain substitution is reduced.

DOI: 10.1103/PhysRevE.65.010703

PACS number(s): 61.30.Eb, 61.30.Cz, 78.35.+c

Chiral smectic liquid crystals exhibiting large electric field-induced tilt angles (or electroclinic effects) are promising materials for electro-optic devices requiring fast, analog switching capability. Recent efforts to improve the application potential of these materials have involved multiple substitution of siloxane groups on the hydrocarbon chains [1,2]. One interesting consequence of this substitution is the absence [3] of the characteristic contraction in layer spacing at the smectic-A to smectic-C\* phase transition. Combined with an unusually large electroclinic effect [3], this result suggests that, in the smectic-A phase of multiply Si-substituted compounds, the molecular cores are already tilted with respect to the layer normal, but are orientationally disordered (a so-called deVries smectic-A). A second unusual feature is the presence of an optical stripe pattern (observed in well oriented samples), whose origin is apparently intrinsic to the material and different in nature from previously observed layer “buckling” stripes [4–6], which occur due to tilt-induced layer contraction in the unsubstituted compounds. Although both lie in the smectic layers, the wave vector of the layer buckling stripes scales inversely with the thickness of samples confined in thin cells [7], while that of the intrinsic stripes is independent of thickness.

Based on these properties and a natural scenario for the development of tilt orientational order in a deVries-type smectic-A, Selinger and others have proposed [8] that the intrinsic stripes are evidence of a chiral modulation of the tilt orientation occurring within the layers. This type of chiral modulation in liquid crystals has been the subject of extensive theoretical study [8–10]. So far, however, in-plane modulated structure in thermotropic smectics has been reported only smectic-C in hexatic phases [11] or within the ferroelectric phase of certain chiral compounds [12].

The present paper reports a light-scattering study of Si-substituted chiral smectics, which provides preliminary evidence of the conjectured phase sequence, smectic-A  $\rightarrow$  modulated smectic-C (or smectic-C<sub>mod</sub>)  $\rightarrow$  uniform smectic-C, for the development of orientational order within the layers of a chiral smectic. In particular, when the number of substituents is increased, we observe anomalous softening and dispersion of the order parameter fluctuations near the smectic-A to smectic-C\* transition. The anomalies can be

explained by a Landau–de Gennes free-energy model of the phase transition, suitably modified [8,9] to allow for the occurrence of an intermediate C<sub>mod</sub> phase.

The general structure of the chiral liquid crystals used in our study is shown in Fig. 1. We will focus on the singly and triply substituted compounds abbreviated 1SiKN105 ( $l=1$ ,  $m=10$ ,  $n=5$  in Fig. 1) and 3SiKN85 ( $l=3$ ,  $m=8$ ,  $n=5$ ). These two compounds differ only in the number of Si substituents on the unbranched alkyl chain. The relevant phase sequences are isotropic–(76.4/76.0)–smectic-A–(66.9/53.5 °C)–smectic-C\* for 1SiKN105/3SiKN85, respectively. Ten micron thick samples were studied in cells treated for “bookshelf” alignment of the smectic layers, with the average layer normal in the substrate plane and parallel to the rubbing direction. Samples were briefly exposed to an applied electric field (5 V/ $\mu$ m) in the vicinity of the isotropic to smectic-A phase transition to assist in achieving an initial monodomain alignment. In the light scattering measurements, the time correlation function of the depolarized scattered intensity ( $\lambda=633$  nm) was measured for scattering vectors  $\vec{q}$  along the layer normal ( $q=q_z$ ) and in the layer plane ( $q=q_x$ ). Temperature scans were performed at fixed  $q_x=7.0 \mu\text{m}^{-1}$  and  $q_z\approx 0$ . Analysis of the measured correlation functions yields the relaxation rates  $\Gamma$  and the scattering amplitudes  $A$  of the director fluctuation modes, with the combination  $(A\Gamma)^{-1}$  being proportional to the generalized viscosity  $\eta$  associated with the damping of these modes [13].

Figure 1 shows depolarized micrographs of the optical texture of 3SiKN85 at temperatures 1.3 °C above and 0.5 °C below the bulk smectic-A to smectic-C\* transition ( $T_{C^*-A}$ ). The smectic layer normal lies in the plane of the figure, parallel to the orientation of the optical stripe pattern. The wave vector of this pattern, which is independent of cell thickness [7], is  $\vec{q}_0=(1.8 \mu\text{m}^{-1})\hat{x}$  at  $T-T_{C^*-A}=1.3$  °C. Just below  $T_{C^*-A}$ , a second, orthogonal pattern of stripes appears with wave number  $\sim 3 \mu\text{m}^{-1}$  along the layer normal ( $\hat{z}$  direction). These are the “dechiralization” lines commonly observed when the helicoidal  $\vec{c}$ -director structure of a C\* phase is suppressed near homogeneous aligning surfaces. A weaker version of the higher temperature stripe texture, with wave number *decreasing* to approximately  $0.6 \mu\text{m}^{-1}$ , is also evident.

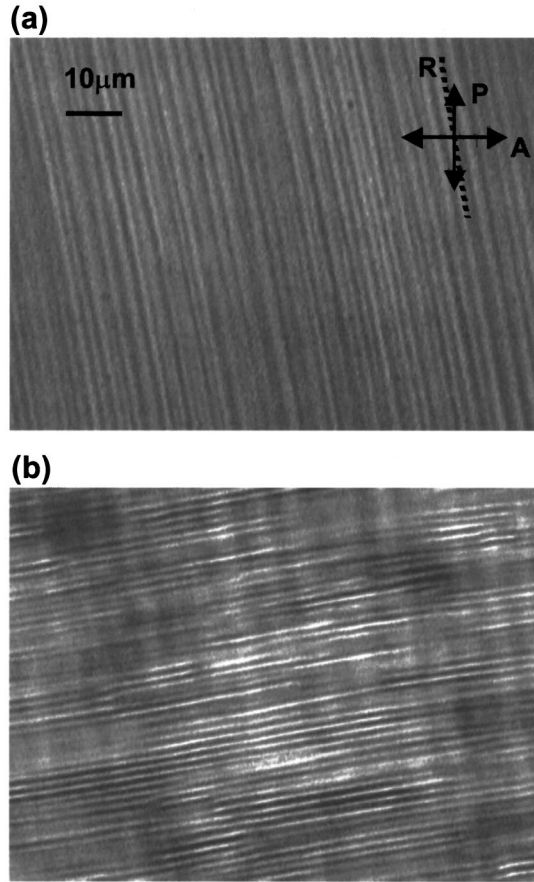
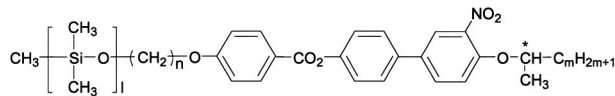


FIG. 1. Chemical structure of the Si-substituted compounds ( $l = 1, 3$ ,  $m = 10, 8$ , and  $n = 5, 5$  for 1SiKN105, 3SiKN85, respectively), and optical stripe textures observed in 3SiKN85 aligned in the “bookshelf” layer geometry. In (a)  $T - T_{AC^*} = 1.3$  °C, and the stripes are approximately parallel to the rub direction (R) of the cell alignment layer and have wave number  $1.8 \mu\text{m}^{-1}$ . In (b), just below the transition to the smectic- $C^*$  phase ( $T - T_{AC^*} = -0.5$  °C), a second, perpendicular stripe pattern appears, indicating the presence of the characteristic helicoidal structure.

Our dynamic light scattering probes bulk fluctuations of the in-plane projection of the optical axis or  $\vec{c}$ -director. Results obtained on the 3SiKN85 sample in Fig. 1 and presented in Figs. 2 and 3 show behavior atypical of normal smectic- $A$  to smectic- $C^*$  transitions. Normally one expects a single diffusive director mode in the disordered (smectic- $A$ ) phase, corresponding to fluctuations in the amplitude of the  $\vec{c}$ -director about zero equilibrium value, and possessing a finite energy gap at  $\vec{q} = 0$  that vanishes at the transition. In a Landau-de Gennes description of the phase transition, the relaxation rate of this “soft” mode is given by  $\Gamma = (a + Kq^2)/\eta$ , where  $a = a_0(T - T_{C^*-A})$  is the temperature-dependent leading coefficient in the Landau-de Gennes expansion of the free-energy density,  $K$  is a Frank elastic con-

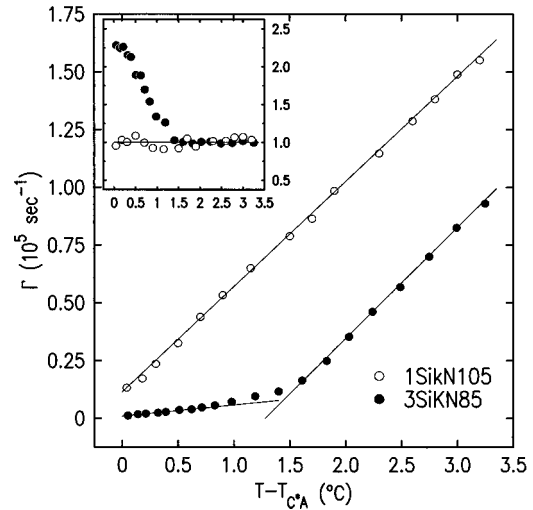


FIG. 2. Temperature dependence of the relaxation rate  $\Gamma$  of the director fluctuations in 1SiKN105 and 3SiKN85. The scattering vector is parallel to the wave vector of the higher temperature modulation (Fig. 1, top) and has a magnitude of  $7.0 \mu\text{m}^{-1}$ . Inset: Temperature dependence of inverse of the fluctuation magnitude  $A$  times  $\Gamma$ , a quantity proportional to the viscosity associated with the fluctuations.

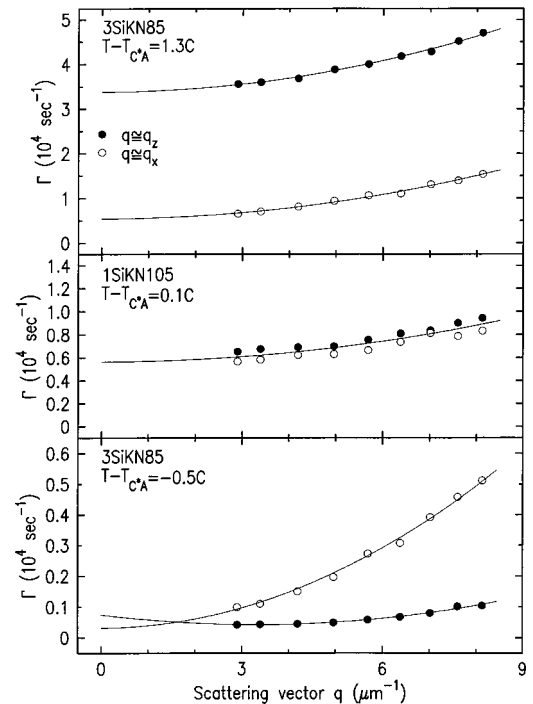


FIG. 3. Dispersion of the director fluctuations in 3SiKN85 for  $T - T_{AC^*} = 1.3$  °C, 1SiKN105 for  $T - T_{AC^*} = 0.1$  °C, and 3SiKN85 for  $T - T_{AC^*} = -0.5$  °C (smectic- $C^*$  phase). Results are presented for scattering vectors along ( $q_x$ ) and perpendicular ( $q_z$ ) to the wave vector of the higher temperature modulation (Fig. 1, top). Solid lines represent a  $q^2$  dependence, except for the  $q_z$  geometry in the smectic- $C^*$  case, where a  $(q_z - q_0)^2$  dependence (with  $q_0 = 3 \mu\text{m}^{-1}$ ) is plotted.

stant for distortion of the director field, and  $\eta$  is a nearly temperature-independent viscosity. The predicted, linear decrease in  $\Gamma$  with temperature and the temperature insensitivity of  $\eta$  have been verified in a number of chiral materials, and, as shown in Fig. 2, hold true in the singly-substituted compound 1SiKN105, where we find  $a_0/\gamma = 4 \times 10^4 \text{ sec}^{-1}\text{-K}^{-1}$ . However, when two additional Si substitutions are made on the same molecule, we observe that, while at higher temperature the slope  $a_0/\eta$  is essentially identical to the value for 1SiKN105, there is a rather abrupt, approximately fivefold decrease in slope beginning at  $T - T_{C^*A} \approx 1.4^\circ\text{C}$ . In addition,  $\eta$  becomes dependent on  $T$  close to the  $C^*$  phase in 3SiKN85.

The dispersion of the director mode in the smectic- $A$  phase of 3SiKN85 also departs significantly from the conventional model. As shown in Fig. 3 (top), just below the crossover observed in the  $T$  dependence of  $\Gamma$ , we find a substantial anisotropy in the gap (value of  $\Gamma$  extrapolated to  $q=0$ ) between the  $q_x$  and  $q_z$  scattering geometries, although the curvature (coefficient of  $q^2$ ) remains quite similar. By contrast, the conventional theory predicts an isotropic gap— $a_0(T - T_{C^*A})$  for both  $q_x$  and  $q_z$ —while allowing for a small variation in curvature (due to elastic constant anisotropy). We again note (Fig. 2, middle) that the singly-substituted 1SiKN105 behaves more conventionally, with nearly zero anisotropy in both gap and curvature even at a temperature very close to the  $A - C^*$  transition.

Now let us briefly review the dynamics of conventional tilted phases—namely, a uniform smectic- $C$  and a helicoidal (out of plane modulated) smectic- $C^*$  phase. For the former, we assume that the equilibrium tilt is along  $\hat{x}$ , so that  $\vec{c}_0 = c_0\hat{x}$  and  $\delta\vec{c} = \delta c_x\hat{x} + \delta c_y\hat{y}$  for the fluctuating part. The normal fluctuation modes [13] are simply  $\delta c_x$ , corresponding to the soft mode, and  $\delta c_y$ , corresponding to the Goldstone mode (rotation of the director about the layer normal). The Goldstone mode is gapless at  $\vec{q} = \vec{0}$ , and, consequently, generally has a much lower relaxation rate than the soft mode. Since the mean-square amplitude varies like  $\Gamma^{-1}$  for hydrodynamic modes, the Goldstone mode has an intrinsically higher scattering cross section. Alternatively, for a helicoidally modulated  $C^*$  phase, the equilibrium  $\vec{c}$ -director becomes  $\vec{c}_0 = c_0 \cos(q_0z)\hat{x} + c_0 \sin(q_0z)\hat{y}$ , where  $\vec{q}_0 = q_0\hat{z}$  is the wave vector of the modulation (along the layer normal). The soft mode corresponds to the combination  $\delta c_x \cos q_0z + \delta c_y \sin q_0z$ , and the Goldstone mode to  $-\delta c_x \sin q_0z + \delta c_y \cos q_0z$ .

Experimentally we measure the time correlation function of the dielectric fluctuations selected by the polarization and wave vectors of the incident and scattered light. For the measurements reported here, when a scattering vector  $q = q_x$  is selected, analysis of the scattering cross section shows that the director fluctuations  $\delta c_x$  and  $\delta c_y$  both contribute significantly. Thus, for a uniform smectic- $C$  phase, the slower (Goldstone) mode (corresponding to  $\delta c_y$ ) should dominate the observed  $q_x$  scattering. On the other hand, when  $q = q_z$ , there should be a much larger contribution from the faster (soft) mode ( $\delta c_x$ ), because in this geometry the rela-

tive scattering from the Goldstone mode is reduced by  $c_0^2$  (which is typically  $\sim 0.1$ ). While the dispersion data in Fig. 3 (top) do indeed reveal slower fluctuations when  $q = q_x$ , extrapolating their dependence on  $q_x^2$  to  $q=0$  still indicates a substantial gap in  $\Gamma$ . This disagrees with the expectation of a vanishing gap at  $\vec{q} = \vec{0}$  for the Goldstone mode in a uniform smectic- $C$  phase. Moreover, the continuing decrease in  $\Gamma$  with decreasing  $T$  observed in Fig. 2 just above the  $C^*$  phase would not be expected if the system was transforming from a uniform ( $C$ ) to helicoidal ( $C^*$ ) structure. In that case, the shift in the dispersion minimum from  $\vec{q} = \vec{0}$  to  $\vec{q} = q_0\hat{z}$  (arising from the modulation of the dielectric tensor along the layer normal  $\hat{z}$ ) should produce a gap and thus *increase* the value of  $\Gamma$  obtained in the  $q_x$  geometry.

For the helicoidal smectic- $C^*$  phase, the Goldstone contains equal contributions from  $\delta c_x$  and  $\delta c_y$ , and thus this mode should dominate both the  $q_x$  and  $q_z$  scattering. Because of the shift in the dispersion minimum to finite  $q_z$ , the relaxation rate for fluctuations with  $q = q_z$  should now be lower than that for  $q = q_x$ , a prediction which indeed agrees with our measurements in Fig. 3 (bottom) just below the transition to the  $C^*$  phase [14], but is opposite from the behavior observed above it.

Next we consider the dynamical effects of an *in-plane* modulation of  $\vec{c}$  (smectic- $C_{mod}$  phase). To calculate these first requires an expression for the equilibrium  $\vec{c}_0$ , which is determined from the Landau–de Gennes free-energy density for a single smectic layer [8,9]:

$$\mathcal{F} = \frac{a}{2} |\vec{c}|^2 + \frac{b}{4} |\vec{c}|^4 + \lambda |\vec{c}|^2 \hat{z} \cdot \vec{\nabla} \times \vec{c} + \frac{K_S}{2} (\vec{\nabla} \cdot \vec{c})^2 + \frac{K_B}{2} (\vec{\nabla} \times \vec{c})^2. \quad (1)$$

Here  $a = a_0(T - T_0)$  and  $T_0$  is the transition from the disordered ( $A$ ) to an ordered ( $C_{mod}$  or uniform  $C$ ) phase, and  $b > 0$  is independent of  $T$ . The third term, allowed by chiral symmetry breaking, couples the magnitude of  $\vec{c}$  to an in-plane modulation of  $\vec{c}$ . In the final terms,  $K_S$  and  $K_B$  are Frank constants for splay and bend distortions of  $\vec{c}$ , respectively. In a one elastic constant model ( $K_S = K_B \equiv K$ ), if  $\sqrt{Kb/2} < \lambda(T) < \sqrt{2Kb}$  for some range  $T_1 < T < T_0$ , where  $T_1$  is given by  $\lambda(T_1) = \sqrt{Kb/2}$ , there are second-order  $A - C_{mod}$  and  $C_{mod} - C^*$  transitions at  $T_0$  and  $T_1$  [9]. (If  $\lambda(T) < \sqrt{Kb/2}$ , there is no stable  $C_{mod}$  phase.)

The Euler-Lagrange equations arising from Eq. (1) have been solved numerically [9], but the analysis can be simplified for temperatures close to the  $C$  phase. Here the solution consists of broad regions in which  $\vec{c}_0$  varies weakly about the value  $\vec{c}_0 = \sqrt{-a/b}\hat{x}$  for a uniform  $C$  phase; these regions are connected by narrow walls in which  $\vec{c}_0$  varies rapidly, but its magnitude is small. Outside the walls, the solution may be written as  $\vec{c}_0 = [\sqrt{-a/b} + \epsilon^2 c_{0x}(x)]\hat{x} + \epsilon c_{0y}(x)\hat{y}$  [9], where  $\epsilon = 2\lambda^2/Kb - 1$  is a temperature dependent parameter that vanishes at the  $C_{mod} - C^*$  transition ( $T = T_1$ ). The functions

$c_{0x}$  and  $c_{0y}$  are expandable in Fourier series with fundamental wave vector  $q_0 = \epsilon q_1$ , where  $q_1$  is a wave number that does not vary strongly near  $T_1$ . Thus  $q_0$  vanishes for  $T \rightarrow T_1$  ( $C_{mod} - C$  transition). Using these results, we find that the Euler-Lagrange equations are satisfied to  $O(\epsilon^2)$  by the truncated series  $c_{0x} = c_0 + c_1 \sin q_0 x + c_0 \cos 2q_0 x$  and  $c_{0y} = c_1 \cos q_0 x$ , with  $c_0 = (\sqrt{-ab/4a})c_1^2$  and  $q_1 = \sqrt{-ab}/\lambda$ . Minimizing the total free energy  $\int \mathcal{F} d\vec{r}$  in  $c_1$ , we then obtain  $c_1^2 = (Kq_1^2/2b)\epsilon$ .

We can now calculate the dynamics close to  $T_1$ , neglecting fluctuations within the narrow walls where  $|\vec{c}_0|$  is small. Inserting our equilibrium expression for  $\vec{c}_0$  plus a fluctuating part  $\delta\vec{c}$  into Eq. (1), taking the Fourier transform, retaining only the lowest-order term in  $\epsilon$  for each quadratic combination  $\delta c_i \delta c_j^*$ , and constructing the phenomenological dynamical equations in the usual way [13], we find

$$\begin{aligned} \eta \delta \dot{c}_x(\vec{q}) &= (2a - Kq^2) \delta c_x(\vec{q}) + i\lambda \sqrt{-\frac{a}{b}} q_x \delta c_y^*(\vec{q}) \\ \eta \delta \dot{c}_y(\vec{q}) &= \left( \frac{3Kab}{4\lambda^2} \epsilon^3 - Kq^2 \right) \delta c_y(\vec{q}) + \frac{3Kab}{8\lambda^2} \epsilon^3 [\delta c_y(\vec{q} + \vec{q}_0) \\ &\quad + \delta c_y(\vec{q} - \vec{q}_0)] - i\lambda \sqrt{-\frac{a}{b}} q_x \delta c_x^*(\vec{q}), \end{aligned} \quad (2)$$

where  $a < 0$ . For small  $q_0$  (near  $T_1$ ), these equations yield two overdamped fluctuation modes, with approximate relaxation rates  $[-2a + Kq^2 - (\lambda^2/2a)q_x^2]/\eta$  and  $[-(Kab/2\lambda^2)\epsilon^3 + Kq^2 + (\lambda^2/2a)q_x^2]/\eta$ , which for  $2|a| \gg \lambda q_x$  correspond to nearly pure order parameter amplitude ( $\sim \delta c_x$ ) and phase ( $\sim \delta c_y$ ) modes, respectively. The important point is that the phase mode in a  $C_{mod}$  phase has a finite gap, which

vanishes (as  $\epsilon^3$ ) at the  $C_{mod}$  to  $C$  phase transition. The gap arises, because, when  $\vec{c}$  and  $\vec{q}_0$  both lie in the layer plane, the orientational order is not invariant to a uniform rotation of  $\vec{c}$  about the layer normal. Equation (2) then accounts for the gap observed for the slower fluctuation mode in Fig. 3, which was measured in a scattering geometry that we have already argued couples primarily to phase fluctuations  $\delta c_y$ . The similarity of the curvature in the dispersion observed for the two scattering geometries in Fig. 3 agrees with our calculated relaxation rates for the modes and the assumption  $2|a| \gg \lambda q_x$  below  $T_0$ . Finally, the distinct temperature dependence of the phase mode gap ( $\sim \epsilon^3$ ) compared to that of the amplitude mode gap ( $\sim a$ ) implies a crossover in the softening of  $\delta c_y$  as one passes from a disordered to modulated phase, which is qualitatively consistent with the behavior observed in Fig. 2.

The bottom panel of Fig. 2 shows that a twofold pretransitional increase in  $\eta$  below  $T - T_{C^*A} \approx 1.3^\circ\text{C}$  also contributes to the slowing down of the fluctuations, but this alone is not enough to account for the observed sevenfold decrease in the relaxation rate over the same range. We note also that the predicted decrease in  $q_0$  as  $T \rightarrow T_1$  is consistent with the textures in Fig. 1, where the wavelength  $2\pi/q_0$  of the higher temperature stripes increases by about three times. We do not, however, observe a vanishing of  $q_0$ , nor a uniform development of the helical pitch lines of the  $C^*$  phase. One possible explanation meriting further investigation is that the higher temperature stripes persist at the surfaces due to a polar interaction with the substrates.

This work was supported by the NSF under Grant No. DMR-9904321. J.N. and B.R. acknowledge support from the Office of Naval Research. We especially thank Jonathan Selinger for several helpful conversations.

- 
- [1] J. Naciri, J. Ruth, G. Crawford, R. Shashidhar, and B.R. Ratna, *Chem. Mater.* **7**, 1397 (1995).
  - [2] B.R. Ratna, G.P. Crawford, S.K. Prasad, J. Naciri, P. Keller, and R. Shashidhar, *Ferroelectrics* **148**, 425 (1993).
  - [3] M.S. Spector, P.A. Heiney, J. Naciri, B. Weslowski, D. Holt, and R. Shashidhar, *Phys. Rev. E* **61**, 1579 (2000).
  - [4] G.P. Crawford, R. Geer, J. Naciri, R. Shashidhar, and B.R. Ratna, *Appl. Phys. Lett.* **65**, 2937 (1994).
  - [5] A.G. Rappaport, P.A. Williams, B.N. Thomas, N.A. Clark, M.B. Ros, and D.M. Walba, *Appl. Phys. Lett.* **67**, 362 (1995).
  - [6] R.E. Geer, S.J. Singer, J.V. Selinger, B.R. Ratna, and R. Shashidhar, *Phys. Rev. E* **57**, 3059 (1998).
  - [7] F.J. Bartoli, J.R. Lindle, S.R. Flom, R. Shashidhar, G. Rubin, J.V. Selinger, and B.R. Ratna, *Phys. Rev. E* **58**, 5990 (1998).
  - [8] J.V. Selinger, J. Xu, R.L.B. Selinger, B.R. Ratna, and R. Shashidhar, *Phys. Rev. E* **61**, 3050 (2000).
  - [9] A.E. Jacobs, G. Goldner, and D. Mukamel, *Phys. Rev. A* **45**, 5783 (1992).
  - [10] G.A. Hinshaw and R. Petschek, *Phys. Rev. A* **39**, 5914 (1989).
  - [11] J.E. MacLennan, U. Sohling, N.A. Clark, and M. Seul, *Phys. Rev. E* **49**, 3207 (1994).
  - [12] E. Gorecka, M. Glogorova, L. Lejcek, and H. Sverenyak, *Phys. Rev. Lett.* **75**, 4047 (1995).
  - [13] I. Drevensek, I. Musevic, and M. Copic, *Phys. Rev. A* **41**, 923 (1990).
  - [14] The solid line for the  $q_z$  data in Fig. 3 represents the expected  $(q_z - q_0)^2$  dispersion of the Goldstone mode in a  $C^*$  phase. There is a residual gap allowed in the solid line because we were not able to probe  $q_z = q_0$  exactly (or much lower  $q_z$ ), due to diffraction coming from the helicoidal modulation. Instead, the experiment was done slightly off the  $q_z$  direction.